



Cite this: *Biomater. Sci.*, 2017, **5**, 1836

Received 13th April 2017,
Accepted 12th June 2017
DOI: 10.1039/c7bm00339k
rsc.li/biomaterials-science

Synthesis of controlled, high-molecular weight poly(L-glutamic acid) brush polymers†

Ryan Baumgartner,^a Diane Kuai^b and Jianjun Cheng  ^{*a,b,c}

We report the synthesis and characterization of high-molecular weight poly(L-glutamic acid) based brush polymers. Utilizing a combination of ring-opening metathesis polymerization of norbornene based monomers and ring-opening polymerization of γ -benzyl-L-glutamate *N*-carboxyanhydride, high-molecular weight γ -benzyl protected poly(L-glutamic acid) brush polymers are synthesized. Controlled and complete deprotection of the benzyl groups using trimethylsilyl iodide resulted in poly(L-glutamic acid) based brush polymers with molecular weights up to 3.6 MDa, which may potentially be used to prepare size-controlled unimolecular polymeric nanomedicine for drug delivery applications. Camptothecin brush poly(L-glutamic acid) conjugates were prepared and their stability, drug release kinetics, and *in vitro* toxicity were studied.

Introduction

Polymer architecture plays an important role in the behavior of a polymer system utilized for drug delivery applications.^{1–6} Due to modern advances in polymer chemistry, new branched architectures including dendrimers,⁷ star,⁸ and brush polymers⁹ have been synthesized with controlled shape and size for applications in the field of nanomedicine.¹⁰ The use of molecular brush polymers in particular is advantageous due to the range of properties that can be tuned, including the side-chain and backbone composition, the grafting density, and the backbone and side-chain length. The broad range of properties that can be tuned allows the polymer architecture to be precisely controlled.^{11–16} Collectively, these properties determine the shape, size, and properties of the polymer and are heavily dependent on the chemistry utilized to construct the polymer. The introduction of ring-opening metathesis polymerization (ROMP)¹⁷ and controlled radical polymerization (CRP)¹⁸ has greatly improved the degree of control over the final brush polymer and has allowed for new delivery

systems that can be tailor-made to a specified shape.^{2,19–22} Furthermore, this chemistry has extended the range of molecular weights (MWs) and thus sizes that can be achieved. Using currently available techniques, the sizes of molecular brush polymers can reach up to the scale of colloids (several hundred nm). Being constructed entirely of covalent bonds, these drug carriers act essentially as unimolecular micelles, which is advantageous as they do not disassemble upon dilution, a problem with polymeric nanomedicine prepared through the self-assembly or aggregation of amphiphilic or hydrophobic polymers.^{23–25} While polymer–drug conjugates possess a stable nano-structure, their sizes are typically very small (<20 nm). The ability to access stable nanomedicine with controlled shape, size, and known stability will be important in understanding the explicit properties of nanomedicine in biological systems.²⁶

In developing new nanomedicine from the bottom-up, however, the synthesis of brush polymers of controlled size and shape still remains challenging. This is due to the limited number of compatible polymerization methods available from which to construct these polymers. As mentioned above, ROMP and CRP have proven to be powerful methods for constructing the polymer backbones utilizing the grafting from, grafting through, and grafting to methods. Most current polymer brushes for drug delivery, however, rely on poly(ethylene glycol) as the main constituent. Grafting through has been widely utilized to access these polymers and thus the length of the polymer side-chains is limited due to the decreased polymerization efficiency at longer macromonomer lengths. Additionally, poly(ethylene glycol) based brush polymers lack the functional handles necessary to attach drugs or other targeting ligands at high loadings. Brush polymers with new compositions remain

^aDepartment of Chemistry, University of Illinois at Urbana-Champaign, Urbana, Illinois 61801, USA. E-mail: jianjunc@illinois.edu; Fax: (+1) 217-333-2736; Tel: (+1) 217-244-3924

^bDepartment of Materials Science and Engineering, University of Illinois at Urbana-Champaign, Urbana, Illinois 61801, USA

^cDepartment of Bioengineering, Beckman Institute for Advanced Science and Technology, Frederick Seitz Materials Research Laboratory, Carl R. Woese Institute for Genomic Biology, University of Illinois at Urbana-Champaign, Urbana, Illinois 61801, USA

†Electronic supplementary information (ESI) available: Experimental details including AFM, CD, acid titration curves, and drug loading data. See DOI: 10.1039/c7bm00339k

rare, as do the controlled methods necessary to synthesize them. Poly(L-glutamic acid) (PGA) is one material that has been recently explored for use in drug delivery systems and is advantageous due to the biocompatibility, biodegradability, and carboxylic acid functional sites.^{27–29} The synthesis of PGA based brush polymers of well-defined architecture and molecular weight, however, has not yet been achieved.

Here, we report the controlled synthesis of brush polymers composed of PGA utilizing a simple one-pot procedure. Our strategy utilizes the controlled ring-opening polymerization (ROP) of γ -benzyl-L-glutamate *N*-carboxyanhydride (BLG-NCA) from a poly(norbornene) (PNB) based macroinitiator, resulting in poly(γ -benzyl-L-glutamate) (PBLG) based brush polymers. Subsequent treatment with trimethylsilyl iodide (TMSI) at room temperature resulted in complete removal of the benzyl groups, providing PGA based brush polymers with controlled molecular weight values and low PDI. We demonstrated that brush polymers composed of PGA with MW up to 3.6 MDa were easily attainable. We subsequently demonstrated the ability to attach a model drug, camptothecin (CPT) to the brush polymers in high loading. These polymers possessed the ability to release drug and showed *in vitro* cytotoxicity toward cancer cells.

Materials and methods

Materials

All solvents and reagents were purchased from Sigma Aldrich and used as received unless otherwise specified. Anhydrous solvents were prepared by passing nitrogen purged solvents through activated alumina columns, and were stored over molecular sieves in the glovebox. γ -Benzyl-L-glutamic acid was purchased from Chem-Impex. All polymerizations were carried out under argon in an MBraun glovebox. All vials used to handle trimethylsilyl (TMS) protected amines were silanized by allowing vials to sit over vapor of chlorotrimethylsilane for 4 h in a desiccator under static vacuum. Vials were rinsed with de-ionized water, dried at 100 °C, and stored in the glovebox. Grubb's 3rd generation catalyst (G3),³⁰ *N*-trimethylsilyl-*cis*-5-norbornene-*exo*-2,3-dicarboxylic anhydride (NB),³¹ γ -benzyl-L-glutamate *N*-carboxyanhydride (Glu-NCA),³¹ and camptothecin-glycine-trifluoroacetic acid (CPT-Gly-TFA)³² were synthesized according to previous procedures.

All cell lines were obtained from ATCC and stored in a cryo-preservation system until needed. The cells were thawed and passaged according to procedures outlined by ATCC. Cells were cultured in Dulbecco's Modified Eagle Medium (DMEM) supplemented with 10% Fetal Bovine Serum (FBS), 1000 units per mL aqueous penicillin G, and 100 μ g per mL streptomycin. 3-(4,5-Dimethylthiazolyl-2)-2,5-diphenyltetrazolium bromide (MTT reagent) was used as purchased from ATCC.

Instrumentation

Nuclear magnetic resonance (NMR) spectra were recorded on a Varian VXR500 or U500 spectrometer. Chemical shifts are

references to residual protons in the deuterated NMR solvents. MestReNova 8.1.1 was used to analyze all spectra. Gel permeation chromatography (GPC) of poly(γ -benzyl-L-glutamate) (PBLG) was performed on a system equipped with a Model 1200 isocratic pump (Agilent Technologies) in series with a 717 Autosampler (Waters) and size exclusion columns (10² Å, 10³ Å, 10⁴ Å, 10⁵ Å, 10⁶ Å Phenogel columns, 5 μ m, 300 \times 7.8 mm, Phenomenex) which were maintained at a temperature of 60 °C. A miniDAWN TREOS (Wyatt Technology) multi-angle laser light scattering (MALLS) operating at a wavelength of 658 nm and an Optilab rEX refractive index detector (Wyatt Technology) operating at a wavelength of 658 nm were used as detectors. The mobile phase consisted of *N,N*-dimethylformamide (DMF) containing 0.1 M LiBr at a flow rate of 1 mL min⁻¹. Prior to injection, polymer solutions were filtered using a 0.45 μ m PTFE filter. Absolute molecular weights of polymers were determined using ASTRA 6.1.1.17 software (Wyatt Technology) and calculated from dn/dc values assuming 100% mass recovery (dn/dc PBLG in DMF + 0.1 M LiBr = 0.0930). Size exclusion chromatography (SEC) and high-performance liquid chromatography (HPLC) were carried out on a Prominence HPLC system (Shimadzu) equipped with a quaternary pump in series with a 20A5 vacuum degasser, a 20A autosampler, a SPD-M20A photo-diode array detector, and a RF-20A fluorescence detector. For SEC analysis, a miniDAWN TREOS MALLS, and Optilab rEX refractive index detector were additionally utilized. SEC separations were performed using a Polysep GFC-P linear column (300 \times 7.8 mm, Phenomenex) using H₂O as the mobile phase at a flow rate of 0.8 mL min⁻¹. Absolute molecular weights of polymers were determined using ASTRA 6.1.1.17 software (Wyatt Technology) and calculated from dn/dc values assuming 100% mass recovery (dn/dc PGA in H₂O = 0.1675). HPLC analysis utilized a Luna Phenyl-Hexyl column (3 μ m, 50 mm \times 4.6 mm, Phenomenex) using a gradient of acetonitrile in H₂O containing 0.1% trifluoroacetic acid at a flow rate of 1.5 mL min⁻¹. Zeta potentials were measured on Malvern Zetasizer. UV-Vis spectroscopy was conducted on either a Nanodrop 2000 (Thermo Fisher Scientific) or a Cary 60 (Agilent). Atomic force microscopy (AFM) was conducted under ambient conditions in tapping mode on a Cypher (Asylum Research) using BS-Tap 300 Al tips (Budget Sensors). Samples were prepared by spin coating a polymer solution (~1 μ g mL⁻¹ in 1.0 mM MgCl₂ in H₂O) onto freshly cleaved mica.

Synthesis of PBLG brush polymers

The synthesis was carried out according to a previous literature protocol.³¹ Briefly, in a glovebox, NB (9.8 mg, 0.0352 mmol) was weighed into a silanized vial and dissolved in dry DCM. A solution of G3 (1 mg mL⁻¹) was added at the desired [M]:[I] ratio such that the final [NB] = 0.02 M. The reaction was stirred at room temperature for 20 minutes per each 100 repeat units and quenched with 10 μ L ethyl vinyl ether. The resulting PNB macroinitiator solutions were stored at -30 °C in the glovebox and used directly.

The PNB-*g*-PBLG brush polymer was then synthesized by dissolving BLG-NCA (60 mg, 0.228 mmol) in DCM in a silanized vial. Then, the PNB macroinitiator solution was added at the desired [M]:[I] ratio at [M] = 0.10 M and stirred for 2–4 hours. Polymers for GPC analysis were prepared by evaporating solvent and dissolving in mobile phase (0.1 M LiBr in DMF).

Synthesis of PGA brush polymers

To PNB-*g*-PBLG solutions (*ca.* 50 mg) in DCM, fresh, colorless trimethylsilyl iodide (TMSI, 195 μ L, 1.37 mmol, 6 equiv. per benzyl group) was added by syringe under a stream of N₂ forming a slightly yellow or red/brown solution. The reaction was stirred at room temperature for 24 hours, and solvent removed *in vacuo*. Saturated NaHCO₃ solution (4 mL) and DI H₂O (4 mL) were added to dissolve the resulting residue and a minimal amount of Na₂S₂O₃ was added to create a colorless solution. Dissolution of the brush polymers was allowed to proceed for 24 h under stirring, resulting in a milky solution. The aqueous phase was washed 3 \times 5 mL with ether to remove benzyl iodide. The resulting solution was transferred to dialysis tubing (50k MWCO) and dialyzed against distilled water for 48 hours. Lyophilization yielded a fluffy white solid in >70% yield (*ca.* 25 mg).

Preparation of CPT-PGA conjugates

In an Eppendorf tube, PNB-PGA (1.0 mg, 7.75 μ mol –COOH) was dissolved in 100 μ L DI water. Proper volumes of fresh, aqueous solutions of 1-ethyl-3-(3-dimethylaminopropyl)carbodiimide hydrochloride (EDC-HCl, 100 mg mL⁻¹, 2.84 μ mol) and *N*-hydroxysuccinimide (NHS, 100 mg mL⁻¹, 2.84 μ mol) were added, followed by the addition of 10.88 μ L of MES buffer (1.0 M, 10 \times). The reaction was allowed to incubate at room temperature for 15 minutes, after which proper volumes of 4-dimethylaminopyridine (DMAP, 50 mg mL⁻¹ in DMF, 0.712 μ mol), CPT-Gly-TFA (10 mg mL⁻¹ in DMF, 0.712 μ mol), and 14.76 μ L PBS buffer (10 \times) was added. The reaction was allowed to sit at room temperature for 48 h. The CPT-PGA conjugate was purified *via* ultrafiltration using 100k MWCO Amicon filters (EMD Millipore), washing with distilled water for a total of 10 spin cycles. Complete removal of free CPT-Gly-TFA was confirmed by analyzing the flow through by UV-Vis spectroscopy. The purified CPT-PGA conjugate was lyophilized, yielding a white powder, and stored in the freezer. For conjugation reactions of varying drug loading, the molar ratio of [EDC-HCl]:[NHS]:[DMAP]:[CPT-Gly] was maintained at 4:4:1:1.

Drug loading and loading efficiency

The number of CPT-Gly molecules attached to the PGA brush polymer was quantified by UV-Vis spectroscopy at a wavelength of 369 nm by comparing against a standard curve. The drug

loading and loading efficiency values were calculated according to the following formula:

$$\text{Drug Loading (wt\%)} = \frac{M_{\text{CPT-Gly}}}{M_{\text{PNB-g-PGA}}} \times 100$$

$$\text{Loading Efficiency (\%)} = \frac{M_{\text{CPT-Gly}}}{M_{\text{CPT-Gly in feed}}} \times 100$$

where $M_{\text{CPT-Gly}}$ refers to the mass of CPT-Gly conjugated to the polymer, $M_{\text{PNB-g-PGA}}$ refers to the mass of the PNB-*g*-PGA brush polymer, and $M_{\text{CPT-Gly in feed}}$ refers to the mass of CPT-Gly added to the conjugation reaction.

Drug release

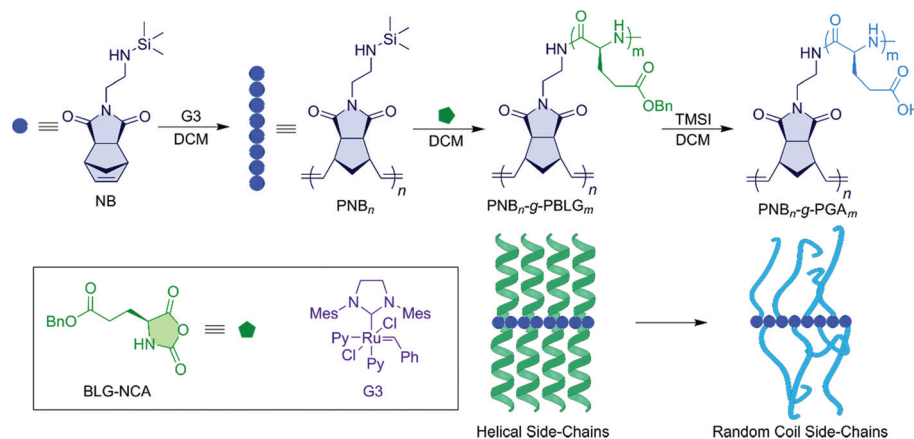
Solutions of CPT-PGA (10 μ g mL⁻¹) were incubated at 37 $^{\circ}$ C in either PBS (pH = 7.4) or acetate (pH = 5.5) buffer. At each time point, an aliquot was removed and analyzed by HPLC to determine the free drug released. The study conducted with three independent replicates.

Cell viability assays

HeLa, LS174T, and HEK cells were plated in a 96-well plate at a cell density of 1000, 5000, and 7000 cells per well for 24 h. The cell media was carefully aspirated and replaced with fresh cell media (100 μ L). Freshly prepared PNB-*g*-PGA, CPT-PGA, or CPT in PBS was added to each well and the cells were incubated for 48 hours at 37 $^{\circ}$ C. The media was then aspirated, the cells were washed with 100 μ L PBS, and replaced with fresh 100 μ L cell media. MTT reagent (10 μ L, 5 mg mL⁻¹ in PBS) was added to each and the cells were incubated for 4 hours at 37 $^{\circ}$ C. The media was aspirated and the cells were washed with 3 \times 100 μ L PBS. Cells and resulting formazan crystals were then dissolved in 100 μ L DMSO, and the absorbance in each well was quantified using a plate reader at λ = 540 nm.

Results and discussion

In order to create PGA based brush polymers that possess varied sizes (or molecular weights) and shapes, we adopted our previously reported method for the synthesis of poly(γ -benzyl-L-glutamate) (PBLG) based brush polymers (Scheme 1).³¹ Compared to other routes utilized to access polypeptide based brush polymers,^{33–37} our method is advantageous for several reasons. First, the synthesis is extremely rapid. In proceeding from the synthesis of the polymer backbone through the final polymerization of the PBLG grafts, less than two hours are required. Second, the synthesis is conducted in dichloromethane, for not only the synthesis of the backbone and side-chain grafts, but also for the deprotection of the benzyl groups. This allows all the reactions to be performed in one pot with no intermediate purification. Last, the methodology we have developed allows us to synthesize brush polymers with ultra-high molecular weights, providing us access to PGA brush polymers of a wide range of sizes and shapes.



Scheme 1 Synthetic route to $\text{PNB}_n\text{-g-PGA}_m$ polymers. Ring-opening metathesis polymerization (ROMP) of NB followed by ring-opening polymerization (ROP) of *N*-carboxyanhydrides and subsequent deprotection of benzyl groups using trimethylsilyl iodide.

We elected to synthesize brush polymers with a range of dimensions to assess what factors might affect the deprotection chemistry, and also to probe what sizes of PGA based brush polymers we could obtain. We began by synthesizing the PNB backbone at $[\text{M}]_0/[\text{I}]_0$ ratios ranging from 50 to 200. This was achieved by polymerizing NB in DCM utilizing Grubbs third generation catalyst (G3). The reaction (which has been described previously³¹) proceeds rapidly and results in polymers of well-controlled molecular weight (MW) and polydispersity index (PDI) values. Following the synthesis of the PNB backbone, the macroinitiator solutions were directly utilized to initiate the polymerization of BLG-NCA. All of the polymerizations were conducted at a relatively low NCA concentration ($[\text{M}]_0 = 0.10 \text{ M}$) to avoid the creation of an overly viscous solution. Even at these relatively low monomer concentrations, the reaction proceeds rapidly, completing in under 1 h with monomer conversion >99%. As expected, the resulting brush polymers possessed accurate MW values and extremely low PDI values, all of which fell below 1.05 (Table 1). The polymer possessing the largest MW value was $\text{PNB}_{100}\text{-g-PBLG}_{200}$ at 4.9 MDa with a polydispersity index (PDI) of 1.02. The GPC traces (Fig. 1a) show monomodal traces that elute earlier with increasing molecular weights. This demonstrates that all of the NCA monomer is initiated from and added to the PNB macroinitiator, ruling out spontaneous initiation and polymerization of NCA that would result in linear polymer.

With the $\text{PNB}_n\text{-g-PBLG}$ brush polymers in hand, we next determined a viable method to remove the benzyl protecting groups and release the water soluble $\text{PNB}_n\text{-g-PGA}$ brush polymers. Previous reports have demonstrated that the most traditionally utilized method of HBr in TFA results in chain cleavage of varying degrees depending on the exact conditions used.^{38,39} Additionally, basic hydrolysis is often accompanied by racemization of the α -carbons along the peptide backbones.²⁷ A mild method utilizing trimethylsilyl iodide (TMSI) appeared to be the most likely for success, as little cleavage has been reported (Scheme 1).^{39,40} We found that reaction of $\text{PNB}_n\text{-g-PBLG}$ at room temperature for 24 h was sufficient to provide complete cleavage of the benzyl protecting groups and minimal to no cleavage of the PNB backbone or polypeptide side-chains. First, SEC analysis of the resulting $\text{PNB}_n\text{-g-PGA}$ polymers in water utilizing UV, multi-angle laser light scattering (MALLS), and refractive index detectors revealed polymers with monomodal peaks that trended towards lower elution volumes with higher MWs (Fig. 1b). This suggests that both backbone and side-chain cleavage is minimal. For $\text{PNB}_{50}\text{-g-PGA}_{200}$ (which possesses an actual side-chain length of 630 due to a grafting density of 30%), the determined MW (2.02 MDa) is close to the expected value of 1.46 MDa suggesting no significant side-chain cleavage (Table 1). Furthermore, polymers having a long backbone such as $\text{PNB}_{200}\text{-g-PGA}_{50}$ also lie close to the expected MW value of 1.77 MDa, having a MW of

Table 1 GPC data for polymers before ($\text{PNB}_n\text{-g-PBLG}_m$) and after ($\text{PNB}_n\text{-g-PGA}_m$) deprotection of the side-chains

Polymer	M_n (M_n^*) ^a /kDa	PDI ^a	Polymer	M_n (M_n^b)/kDa	PDI ^b
$\text{PNB}_{50}\text{-g-PBLG}_{25}$	366 (274)	1.05	$\text{PNB}_{50}\text{-g-PGA}_{25}$	230 (220)	1.38
$\text{PNB}_{50}\text{-g-PBLG}_{50}$	694 (548)	1.03	$\text{PNB}_{50}\text{-g-PGA}_{50}$	450 (410)	1.16
$\text{PNB}_{100}\text{-g-PBLG}_{50}$	1460 (1100)	1.03	$\text{PNB}_{100}\text{-g-PGA}_{50}$	700 (860)	1.12
$\text{PNB}_{50}\text{-g-PBLG}_{200}$	2470 (2200)	1.01	$\text{PNB}_{50}\text{-g-PGA}_{200}$	2020 (1460)	1.25
$\text{PNB}_{200}\text{-g-PBLG}_{50}$	3000 (2200)	1.04	$\text{PNB}_{200}\text{-g-PGA}_{50}$	1920 (1770)	1.35
$\text{PNB}_{100}\text{-g-PBLG}_{200}$	4860 (4400)	1.02	$\text{PNB}_{100}\text{-g-PGA}_{200}$	3620 (2860)	1.06

M_n^* = Expected molecular weight. ^a Determined by GPC in 0.1 M LiBr in DMF. ^b Determined by SEC in H_2O .

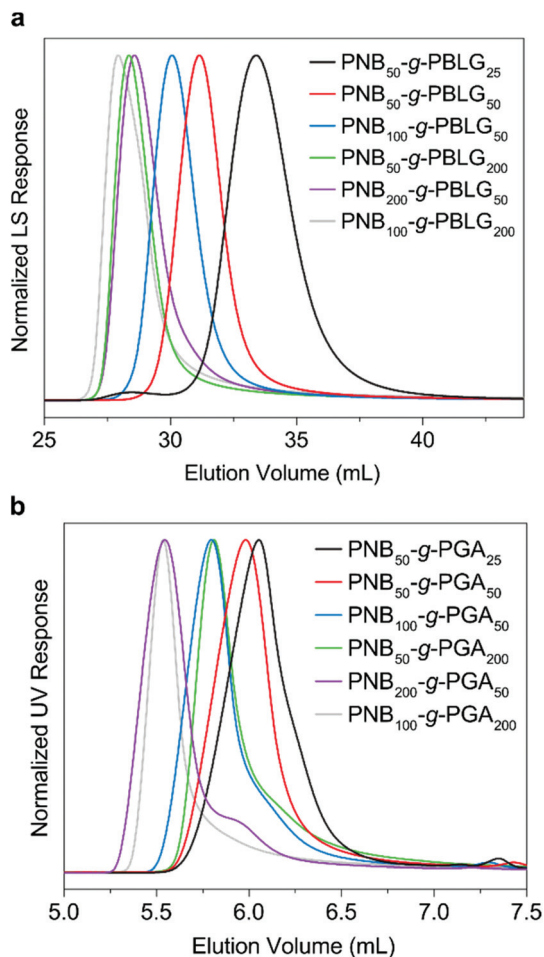


Fig. 1 a. GPC-LS traces of PNB-g-PBLG brush polymers. b. SEC traces of PNB-g-PGA brush polymers after deprotection of the benzyl groups.

1.92 MDa. For this polymer, however, a shoulder at longer retention times is noticed, suggesting that the PNB backbone may be susceptible to cleavage by TMSI, as shorter backbone lengths of 100 and 50 did not show this feature. The PDI values of the deprotected brush polymers are slightly higher than the PBLG based precursors, yet remain relatively low. For instance, the polymer with the highest PDI value is PNB₅₀-g-PGA₂₅ at 1.38. For the majority of the polymers synthesized,

however, the PDI values fall between 1.1 and 1.3, again, suggesting a minimal degree of side reactions or cleavage during the deprotection reaction. Thus, from the SEC data of the deprotected polymers, we have demonstrated the successful synthesis of PGA based brush polymers with MW values up to 3.6 MDa.

Visualization using atomic force microscopy (AFM) was also conducted to confirm the size and shape of the resulting PGA based brush polymers. Visualization of the PGA brush polymers was hindered due to the tendency of the polymers to aggregate, especially for the polymers possessing longer backbones (Fig. S1†). Additionally, due to poor adhesion of the polymers to highly oriented pyrolytic graphite (HOPG) or bare mica when spin coated from water, MgCl₂ was utilized to aid adhesion. Under optimized conditions, PNB₅₀-g-PGA₅₀ was observed to possess a rod-like structure (Fig. 2a), in analogy to their benzyl protected precursors.³¹ The polymers had an average length of 47 nm and a length polydispersity (L_w/L_n) of 1.30 (Fig. 2c). The measured length is higher than expected, as the PNB backbone in the fully extended conformation is expected to have a length of ~35 nm (~0.7 nm per NB). From previous studies of PBLG brush polymers, the grafting density was found to be ~20% for PBLG side-chains of designed DP = 50, suggesting a contracted backbone conformation.³¹ Length measurements of these PBLG polymers by AFM supported this contention revealing backbone lengths that were shorter than expected. The longer lengths and higher length dispersity values for the deprotected PGA brush polymers are, instead, likely due a combination of effects stemming from geometric effects of the AFM tips, charge repulsion of the carboxylic acid groups, and aggregation of the polymer brushes.

The AFM height data may also support the conformational transition of the α -helical side-chains of PBLG into the random coil structure of PGA. PBLG based brush polymers with α -helical structure have heights near ~3.0 nm which corresponds to the width of ~2 α -helices.³¹ After removal of the benzyl groups, the Z-average height of the brushes was reduced to 0.8 ± 0.1 nm which is less than the width of an α -helix (Fig. 2b). It is important to note here, however, that circular dichroism (CD) measurements of the PGA brush polymers in water reveal a random coil structure, whereas a structure with a low degree of helicity (20%) is present in the presence of magnesium cations (Fig. S2†).⁴¹

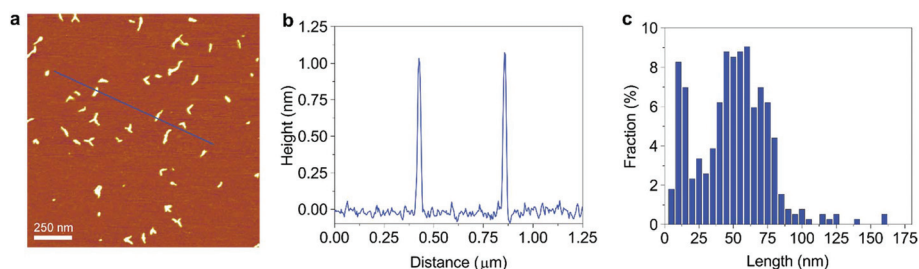


Fig. 2 a–c. AFM height image (a), height profile (b) and length histogram ($n = 104$) (c) of deprotected PNB₅₀-g-PGA₅₀ brush polymers spin coated from 1.0 mM MgCl₂ on mica.

In order to confirm complete removal of the benzyl groups from the polymer side-chains, ^1H NMR analysis was conducted in D_2O . The peaks typical of PGA were clearly evident at δ 4.29, 2.43, and 2.06 ppm, in a ratio of 1 : 2 : 2, respectively (Fig. 3a). Notably, however, there were no aromatic signals in the spectrum suggesting complete removal of the benzyl groups. UV-Vis analysis of the PGA based brush polymers also suggested the absence of any benzyl groups, evidenced by the lack of absorbance near 252 nm (Fig. 3b).

For biological applications, the control over the size and the excellent solubility and solution stability of these materials suggests their advantageous use as a drug carrier. Indeed, linear PGA based drug carriers have been successfully utilized already. With this goal in mind, we investigated the utility of the PGA based brush polymers to solubilize, carry, and release the cytotoxic topoisomerase inhibitor camptothecin (CPT). Initially, we were concerned with the terminal amines of the PGA chains that might lead to crosslinking and aggregation of the brush polymers. Our experience, however, in attempting to utilize these amines for conjugation reactions with isothiocyanate based dyes led to no conjugation, suggesting that the terminal groups have cyclized to form pyroglutamic acid moieties. It was then straightforward to carry out our initial attempts to conjugate CPT directly to the side-chain carboxylate groups of PGA. Utilizing the hydroxyl group of CPT to form an ester bond with PGA provided poor conjugation efficiency using 1-ethyl-3-(3-dimethylaminopropyl)carbodiimide (EDC) *N*-hydroxysuccinimide (NHS) coupling, likely due to the sterically hindered tertiary alcohol of CPT.^{28,42} Instead, modifying CPT with a glycine linker (CPT-Gly) on the 20-OH position resulted in a much more efficient conjugation reaction due to the decreased steric hindrance at the drug site, and the nucleophilic amine of the glycine (Fig. 4a). Under optimal coupling conditions we were able to achieve up to 27 wt% loading of CPT-Gly onto the PGA brush polymers resulting in a loading efficiency of 73%, identical to experiments performed with linear PGA_{90} under identical conditions (Table S1†). The resulting CPT-PGA brush polymers still maintained excellent aqueous solubility at these loadings of CPT-Gly. We attempted higher drug loading, however, both the loading of drug and loading efficiency decreased due to precipitation of the NHS ester of the PGA brush polymers during conjugation (Table S1†). Yields of the final polymers after purification and lyophilization were quantitative. The new CPT-PGA based

brush polymers were confirmed by UV-Vis spectroscopy to possess an absorbance profile consistent with intact CPT (Fig. 3b).

The ζ -potential of the brush polymers was also measured at basic, neutral, and acidic pH values (Fig. 4b). Under mildly basic pH conditions (pH = 8.5), the ζ -potential of the polymers was measured at -51 mV, suggesting a stable solution of polymer brushes. As the pH was lowered to physiological conditions (pH = 7.4) the ζ -potential decreased to -33 mV. Further decreasing the pH to 5.5 at which the polymers still maintained good solubility resulted in an additional decrease in the ζ -potential to -23 mV, suggesting a decrease in colloidal stability. These values agree well with the measured pK_a of the PGA brush polymer which was measured to be 5.3 (Fig. S3†). This pK_a value is slightly higher than the measured pK_a of the linear polymer, which possessed a value of 4.9, likely due to the increased charge repulsion upon deprotonation in the brush polymer architecture.

Release of the final drug from the PGA carrier is necessary for the drug to reach its target in the active form. The kinetics of this release and the form of the released drug are crucial during this process. For these reasons, we monitored the kinetics of CPT release under both physiological pH (7.4) and acidic pH (5.5) which is encountered in tumor tissues (Fig. 4c). The release of drug from CPT-PGA occurred over the course of one month under these conditions, and occurred *via* ester hydrolysis. The release of drug under neutral conditions occurred at a faster release rate, possessing a pseudo-first order rate constant of $1.18 \times 10^{-6} \text{ s}^{-1}$. The release under acidic conditions occurred over $3\times$ slower, at a rate of $3.32 \times 10^{-7} \text{ s}^{-1}$. These values correspond to a half-lives of 6.8 and 24 days, respectively. The slower release at acidic pH values is consistent with previous data for CPT-Gly based drug conjugates utilizing polymers such as β -cyclodextrin and HPMA.^{43,44} The timescale for release is longer than PEG³² or β -cyclodextrin⁴³ based conjugates of CPT-Gly, but shorter than linear PGA conjugated to CPT.⁴⁵ Additionally, the release of the free, intact CPT drug was confirmed *via* HPLC analysis confirming that hydrolysis occurred only at the ester site of the CPT-PGA conjugate (Fig. 4d).

To confirm that these CPT-PGA drug conjugates are capable of killing tumor cells, we conducted cell viability assays, comparing the PGA brush polymer carrier alone, CPT-PGA, and free CPT (Fig. 5). The MTT viability assay of the PGA

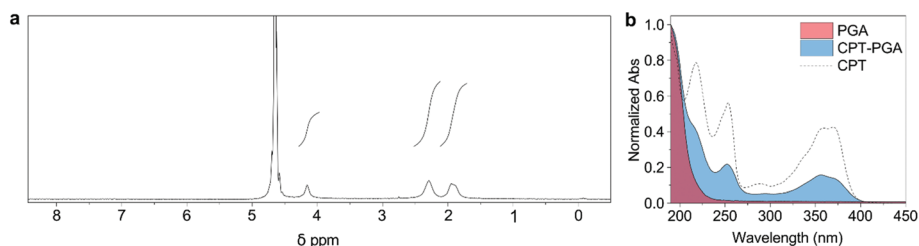


Fig. 3 a. ^1H NMR of $\text{PNB}_{50}\text{-g-PGA}_{50}$ brush polymer in D_2O . b. UV-Vis spectrum of $\text{PNB}_{50}\text{-g-PGA}_{50}$ (red), CPT-PGA (blue) and free CPT (dotted).

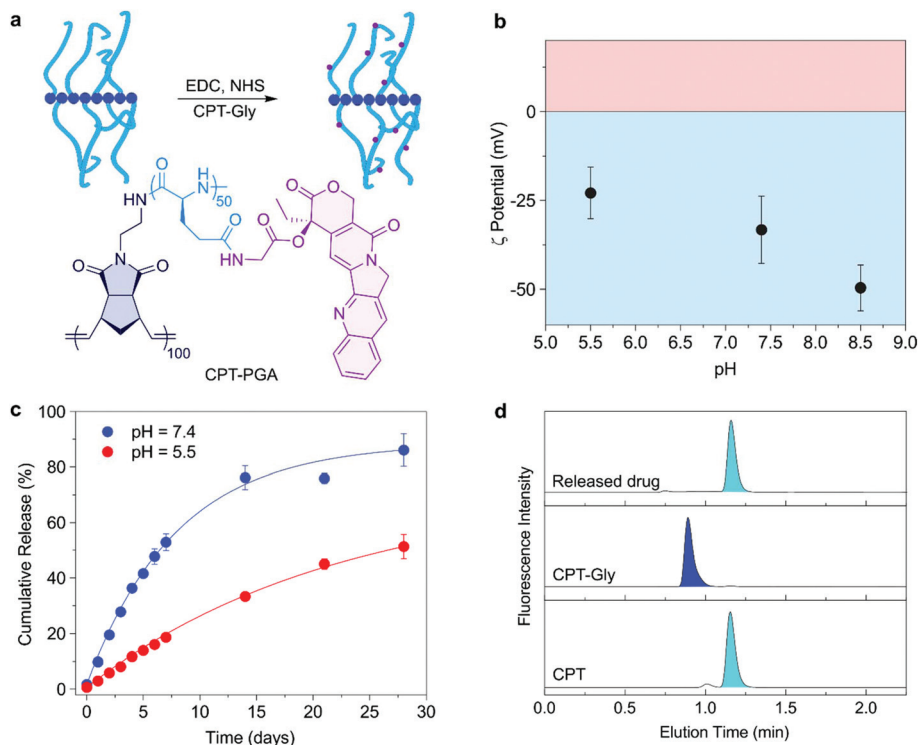


Fig. 4 a. Conjugation scheme for attaching CPT-Gly to PNB₅₀-g-PGA₅₀ forming CPT-PGA. b. ζ -Potential of PNB₅₀-g-PGA₅₀ at various pH values. c. Release of CPT from CPT-PGA at pH = 7.4 and 5.5 over the course of 30 days at 37 °C. d. HPLC fluorescence chromatograms of CPT, CPT-Gly, and drug released from CPT-PGA, demonstrating drug is released as native CPT.

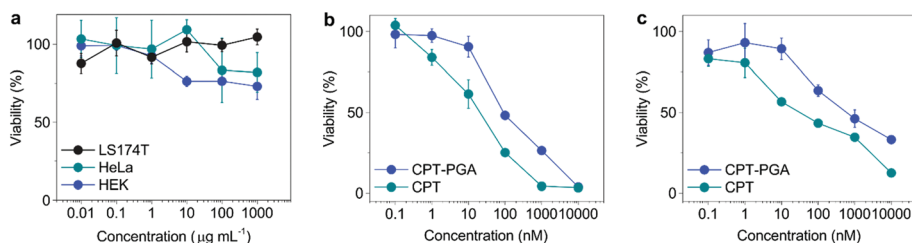


Fig. 5 a. MTT toxicity profiles of PNB₅₀-g-PGA₅₀ on LS174T, HeLa, and HEK cells. b. MTT viability assay of CPT-PGA and CPT on HeLa cells. c. MTT viability assay of CPT-PGA and CPT on LS174T cells. Error bars refer to standard deviations of $n = 5$ independent replicates.

brushes alone confirmed low cytotoxicity at values as high as 1 mg mL^{-1} for HeLa, LS174T, and HEK cell lines. When the HeLa and LS174T cancer cell lines were tested against the CPT-PGA based carriers, a dose dependent response was observed that followed the trend of free CPT itself. For LS174T cells, the CPT-PGA had an IC_{50} of 560 nM, with CPT having an IC_{50} of 30 nM. In HeLa cells, these values are 85 nM and 20 nM for CPT-PGA and CPT, respectively.

Conclusion

In conclusion, we have shown that utilizing the controlled polymerization chemistry performed in chlorinated solvents, we are able to synthesize large MW PBLG based brush polymers and deprotect them completely forming PGA based

brush polymers, with MW values up to 3.6 MDa. This polymerization chemistry affords polymers with PDI values typically between 1.2 and 1.3. We then demonstrated the ability of these large MW polymers to act as unimolecular nanocarriers for CPT, efficiently solubilizing and releasing the drug in its native form. The PGA brush polymers themselves are non-toxic to cells, yet the CPT-PGA brush polymers show cytotoxicity, demonstrating the potential of these carriers for applications in drug delivery.

Author contributions

The manuscript was written through contributions of all authors. All authors have given approval to the final version of the manuscript.

Conflict of interest

The authors declare no competing financial interest.

Acknowledgements

This work was supported by the National Science Foundation (DMR-1309525) and the National Institute of Health (R21 1R21AI117080).

References

- 1 L. Y. Qiu and Y. H. Bae, Polymer architecture and drug delivery, *Pharm. Res.*, 2006, **23**, 1–30.
- 2 M. Müllner, S. J. Dodds, T.-H. Nguyen, D. Senyschyn, C. J. H. Porter, B. J. Boyd and F. Caruso, Size and rigidity of cylindrical polymer brushes dictate long circulating properties in vivo, *ACS Nano*, 2015, **9**, 1294–1304.
- 3 S. Venkataraman, J. L. Hedrick, Z. Y. Ong, C. Yang, P. L. R. Ee, P. T. Hammond and Y. Y. Yang, The effects of polymeric nanostructure shape on drug delivery, *Adv. Drug Delivery Rev.*, 2011, **63**, 1228–1246.
- 4 P. Decuzzi, B. Godin, T. Tanaka, S. Y. Lee, C. Chiappini, X. Liu and M. Ferrari, Size and shape effects in the bio-distribution of intravascularly injected particles, *J. Controlled Release*, 2010, **141**, 320–327.
- 5 J. Burke, R. Donno, R. d'Arcy, S. Cartmell and N. Tirelli, The effect of branching (star architecture) on poly(D,L-lactide) (pdlla) degradation and drug delivery, *Biomacromolecules*, 2017, **18**, 728–739.
- 6 J.-M. Williford, J. L. Santos, R. Shyam and H.-Q. Mao, Shape control in engineering of polymeric nanoparticles for therapeutic delivery, *Biomater. Sci.*, 2015, **3**, 894–907.
- 7 P. Kesharwani, K. Jain and N. K. Jain, Dendrimer as nano-carrier for drug delivery, *Prog. Polym. Sci.*, 2014, **39**, 268–307.
- 8 W. Wu, W. Wang and J. Li, Star polymers: Advances in biomedical applications, *Prog. Polym. Sci.*, 2015, **46**, 55–85.
- 9 M. Müllner, Molecular polymer brushes in nanomedicine, *Macromol. Chem. Phys.*, 2016, **217**, 2209–2222.
- 10 A. Duro-Castano, J. Movellan and M. J. Vicent, Smart branched polymer drug conjugates as nano-sized drug delivery systems, *Biomater. Sci.*, 2015, **3**, 1321–1334.
- 11 A. Li, Z. Li, S. Zhang, G. Sun, D. M. Policarpio and K. L. Wooley, Synthesis and direct visualization of dumbbell-shaped molecular brushes, *ACS Macro Lett.*, 2012, **1**, 241–245.
- 12 J. Burdyńska, W. Daniel, Y. Li, B. Robertson, S. S. Sheiko and K. Matyjaszewski, Molecular bottlebrushes with bimodal length distribution of side chains, *Macromolecules*, 2015, **48**, 4813–4822.
- 13 J. Bolton and J. Rzyzewski, Synthesis and melt self-assembly of ps-pmma-pla triblock bottlebrush copolymers, *Macromolecules*, 2014, **47**, 2864–2874.
- 14 P. J. M. Stals, Y. Li, J. Burdyńska, R. Nicolaÿ, A. Nese, A. R. A. Palmans, E. W. Meijer, K. Matyjaszewski and S. S. Sheiko, How far can we push polymer architectures?, *J. Am. Chem. Soc.*, 2013, **135**, 11421–11424.
- 15 M. Schappacher and A. Deffieux, Synthesis of macrocyclic copolymer brushes and their self-assembly into supramolecular tubes, *Science*, 2008, **319**, 1512.
- 16 Y. Guo, J. D. van Beek, B. Zhang, M. Colussi, P. Walde, A. Zhang, M. Kröger, A. Halperin and A. Dieter Schlüter, Tuning polymer thickness: Synthesis and scaling theory of homologous series of dendronized polymers, *J. Am. Chem. Soc.*, 2009, **131**, 11841–11854.
- 17 S. Jha, S. Dutta and N. B. Bowden, Synthesis of ultralarge molecular weight bottlebrush polymers using grubbs' catalysts, *Macromolecules*, 2004, **37**, 4365–4374.
- 18 K. L. Beers, S. G. Gaynor, K. Matyjaszewski, S. S. Sheiko and M. Möller, The synthesis of densely grafted copolymers by atom transfer radical polymerization, *Macromolecules*, 1998, **31**, 9413–9415.
- 19 H. Unsal, S. Onbulak, F. Calik, M. Er-Rafik, M. Schmutz, A. Sanyal and J. Rzyzewski, Interplay between molecular packing, drug loading, and core cross-linking in bottlebrush copolymer micelles, *Macromolecules*, 2017, **50**, 1342–1352.
- 20 J. A. Johnson, Y. Y. Lu, A. O. Burts, Y.-H. Lim, M. G. Finn, J. T. Koberstein, N. J. Turro, D. A. Tirrell and R. H. Grubbs, Core-clickable peg-branch-azide bivalent-bottle-brush polymers by romp: Grafting-through and clicking-to, *J. Am. Chem. Soc.*, 2010, **133**, 559–566.
- 21 J. Liu, A. O. Burts, Y. Li, A. V. Zhukhovitskiy, M. F. Ottaviani, N. J. Turro and J. A. Johnson, "Brush-first" method for the parallel synthesis of photocleavable, nitroxide-labeled poly(ethylene glycol) star polymers, *J. Am. Chem. Soc.*, 2012, **134**, 16337–16344.
- 22 J. Zou, Y. Yu, Y. Li, W. Ji, C.-K. Chen, W.-C. Law, P. N. Prasad and C. Cheng, Well-defined diblock brush polymer-drug conjugates for sustained delivery of paclitaxel, *Biomater. Sci.*, 2015, **3**, 1078–1084.
- 23 H. Chen, S. Kim, L. Li, S. Wang, K. Park and J.-X. Cheng, Release of hydrophobic molecules from polymer micelles into cell membranes revealed by Förster resonance energy transfer imaging, *Proc. Natl. Acad. Sci. U. S. A.*, 2008, **105**, 6596–6601.
- 24 H. Chen, S. Kim, W. He, H. Wang, P. S. Low, K. Park and J.-X. Cheng, Fast release of lipophilic agents from circulating peg-pdlla micelles revealed by in vivo Förster resonance energy transfer imaging, *Langmuir*, 2008, **24**, 5213–5217.
- 25 K. C. Liu and Y. Yeo, Extracellular stability of nanoparticulate drug carriers, *Arch. Pharmacol. Res.*, 2014, **37**, 16–23.
- 26 L. Tang, X. Yang, Q. Yin, K. Cai, H. Wang, I. Chaudhury, C. Yao, Q. Zhou, M. Kwon, J. A. Hartman, I. T. Dobrucki, L. W. Dobrucki, L. B. Borst, S. Lezmi, W. G. Helfferich, A. L. Ferguson, T. M. Fan and J. Cheng, Investigating the optimal size of anticancer nanomedicine, *Proc. Natl. Acad. Sci. U. S. A.*, 2014, **111**, 15344–15349.

- 27 C. Li, Poly(l-glutamic acid)-anticancer drug conjugates, *Adv. Drug Delivery Rev.*, 2002, **54**, 695–713.
- 28 J. W. Singer, P. De Vries, R. Bhatt, J. Tulinsky, P. Klein, C. Li, L. Milas, R. A. Lewis and S. Wallace, Conjugation of camptothecins to poly-(l-glutamic acid), *Ann. N. Y. Acad. Sci.*, 2000, **922**, 136–150.
- 29 A. Duro-Castano, I. Conejos-Sánchez and J. M. Vicent, Peptide-based polymer therapeutics, *Polymers*, 2014, **6**, 515–551.
- 30 M. S. Sanford, J. A. Love and R. H. Grubbs, A versatile precursor for the synthesis of new ruthenium olefin metathesis catalysts, *Organometallics*, 2001, **20**, 5314–5318.
- 31 R. Baumgartner, H. Fu, Z. Song, Y. Lin and J. Cheng, Cooperative polymerization of α -helices induced by macromolecular architecture, *Nat. Chem.*, 2017, **9**, 614–622.
- 32 R. B. Greenwald, A. Pendri, C. D. Conover, C. Lee, Y. H. Choe, C. Gilbert, A. Martinez, J. Xia, D. Wu and M.-m. Hsue, Camptothecin-20-peg ester transport forms: The effect of spacer groups on antitumor activity, *Bioorg. Med. Chem.*, 1998, **6**, 551–562.
- 33 H. Lu, J. Wang, Y. Lin and J. Cheng, One-pot synthesis of brush-like polymers via integrated ring-opening metathesis polymerization and polymerization of amino acid n-carboxyanhydrides, *J. Am. Chem. Soc.*, 2009, **131**, 13582–13583.
- 34 A. J. Rhodes and T. J. Deming, Tandem catalysis for the preparation of cylindrical polypeptide brushes, *J. Am. Chem. Soc.*, 2012, **134**, 19463–19467.
- 35 B. Zhang, K. Fischer and M. Schmidt, Cylindrical polypeptide brushes, *Macromol. Chem. Phys.*, 2005, **206**, 157–162.
- 36 Z. Wei, S. Zhu and H. Zhao, Brush macromolecules with thermo-sensitive coil backbones and pendant polypeptide side chains: Synthesis, self-assembly and functionalization, *Polym. Chem.*, 2015, **6**, 1316–1324.
- 37 M. Sahl, S. Muth, R. Branscheid, K. Fischer and M. Schmidt, Helix-coil transition in cylindrical brush polymers with poly-l-lysine side chains, *Macromolecules*, 2012, **45**, 5167–5175.
- 38 E. R. Blout and M. Idelson, Polypeptides. Vi. Poly- α -l-glutamic acid: Preparation and helix-coil conversions, *J. Am. Chem. Soc.*, 1956, **78**, 497–498.
- 39 J. Han, J. Ding, Z. Wang, S. Yan, X. Zhuang, X. Chen and J. Yin, The synthesis, deprotection and properties of poly (γ -benzyl-l-glutamate), *Sci. China: Chem.*, 2013, **56**, 729–738.
- 40 G. Subramanian, R. P. Hjelm, T. J. Deming, G. S. Smith, Y. Li and C. R. Safinya, Structure of complexes of cationic lipids and poly(glutamic acid) polypeptides: A pinched lamellar phase, *J. Am. Chem. Soc.*, 2000, **122**, 26–34.
- 41 J. A. Morrow, M. L. Segall, S. Lund-Katz, M. C. Phillips, M. Knapp, B. Rupp and K. H. Weisgraber, Differences in stability among the human apolipoprotein e isoforms determined by the amino-terminal domain, *Biochemistry*, 2000, **39**, 11657–11666.
- 42 R. Bhatt, P. de Vries, J. Tulinsky, G. Bellamy, B. Baker, J. W. Singer and P. Klein, Synthesis and in vivo antitumor activity of poly(l-glutamic acid) conjugates of 20(s)-camptothecin, *J. Med. Chem.*, 2003, **46**, 190–193.
- 43 J. Cheng, K. T. Khin, G. S. Jensen, A. Liu and M. E. Davis, Synthesis of linear, β -cyclodextrin-based polymers and their camptothecin conjugates, *Bioconjugate Chem.*, 2003, **14**, 1007–1017.
- 44 V. R. Caiolfa, M. Zamai, A. Fiorino, E. Frigerio, C. Pellizzoni, R. d'Argy, A. Ghiglieri, M. G. Castelli, M. Farao, E. Pesenti, M. Gigli, F. Angelucci and A. Suarato, Polymer-bound camptothecin: Initial biodistribution and antitumour activity studies, *J. Controlled Release*, 2000, **65**, 105–119.
- 45 Y. Zou, Q. P. Wu, W. Tansey, D. Chow, C. Charnsangavej, S. Wallace and C. Li, Effectiveness of water soluble poly(l-glutamic acid)-camptothecin conjugate against resistant human lung cancer xenografted in nude mice, *Int. J. Oncol.*, 2001, **18**, 331–336.